Near Infrared Broadband Emission and Spectroscopic Properties of Tm^{3+}/Nd^{3+} Codoped Optical Fiber

Lin Htein[1], Pramod R. Watekar[2], Weiwei Fan[3], Seongmin Ju[3],
Bok Hyeon Kim[4] and Won-Taek Han[1,3]

[1]*Department of Photonics and Applied Physics, Gwangju Institute of Science and Technology, Gwangju 500-712, South Korea*

[2]*Sterlite Technologies Limited, Waluj, Aurangabad 431136, India*

[3]*School of Information and Communications, Gwangju Institute of Science and Technology, Gwangju 500-712, South Korea*

[4]*Advanced Photonics Research Institute, Gwangju Institute of Science and Technology, Gwangju 500-712, South Korea*

Keywords: Broadband Fiber Laser, Codoped Optical Fiber, Energy Transfer, Near Infrared Emission, Nd^{3+}, Tm^{3+}, Spectroscopic Properties.

Abstract: The emission bands at 934, 1083, 1279, 1362, 1414 and 1720 nm were found to appear from the Tm^{3+}/Nd^{3+} codoped optical fiber upon excitation at 633 nm. Near infrared emissions of Tm^{3+} at 1279, 1414 and 1720 nm confirmed a very efficient energy transfer (ET) between Tm^{3+} and Nd^{3+} ions. Since the emission band of Nd^{3+} at 1362 nm helped to bridge the wavelength gap between the emission peaks of Tm^{3+} at 1279 and 1414 nm, the ET process made the Tm^{3+}/Nd^{3+} codoped fiber applicable in broadband fiber laser operating around 1215–1515 nm. Further, cross-sections for the respective bands, spectroscopic properties and nonlinear characteristics of the Tm^{3+}/Nd^{3+} codoped fiber were investigated.

1 INTRODUCTION

Because of the impact of wavelength division multiplexing (WDM) telecommunication systems, broadband light source and broadband amplifier have been received growing attention in world-wide optical communication (Tanabe, 2002). Nonetheless, rare-earth (RE) ions, so widely used as laser-active media in optical fiber, commonly have narrow absorption and emission bands arising from the parity-forbidden *4f-4f* transitions (Zabicky, 2009). In order to broaden the emission bandwidth, the most attractive method is that RE ions are codoped into the core of the fiber where the energy transfer (ET) process takes place between different species of ions (Tanabe, 2002). Moreover, such ET process favours emission efficiency and enhances the gain of an amplifier (Brandão et al., 2006).

The present work, codoping Nd^{3+} as a sensitizer for Tm^{3+} in the core of the fiber, was concerned with the needs of broadband fiber laser and amplifier for future optical communication. The motivation for our investigation was that the emission of Nd^{3+} around 1340 nm can fill the wavelength gap complementing the emission of Tm^{3+} in short wavelength band (S-band, 1460–1530 nm) (Shen et al., 2002). Moreover, since two excited levels, i.e., Nd^{3+}: $^4F_{3/2}$ and Tm^{3+}: $^3H_4$, are well matched (Tanabe et al., 2000), the ET process is likely to occur and the lifetime of the Nd^{3+} at $^4F_{3/2}$ level is long enough to induce efficient ET. And, the large absorption cross-section of Nd^{3+} around 600 nm provides powerful absorption for effective pumping with commercially available lasers (Zhang et al., 2010).

Although the enhancement of upconversion emission efficiency by using Nd^{3+} as a sensitizer for Tm^{3+} (Rakov et al., 2009); (Rakov et al., 2002) and the ET process between them (Brandão et al., 2006); (Chung and Heo, 200); (Lahoz et al., 2008); (Tanabe et al., 2000) were reported in different host materials, no broadband near infrared (NIR) emission of Tm^{3+}/Nd^{3+} codoped silicate optical fiber was investigated. In this study, a wide range of NIR emission spectrum broadening from 1215 to 1515 nm with FWHM of 158 nm has been studied in Tm^{3+}/Nd^{3+} codoped fiber upon exciting at 633 nm.

Htein L., R. Watekar P., Fan W., Ju S., Hyeon Kim B. and Han W..
Near Infrared Broadband Emission and Spectroscopic Properties of Tm3+/Nd3+ Codoped Optical Fiber.
DOI: 10.5220/0004338200250032
In *Proceedings of the International Conference on Photonics, Optics and Laser Technology* (PHOTOPTICS-2013), pages 25-32
ISBN: 978-989-8565-44-0

Further, the spectroscopic parameters of the Tm^{3+}/Nd^{3+} codoped fiber was determined by applying the Judd-Ofelt (JO) analysis. Furthermore, cross-sections for the respective bands were investigated and consequently its nonlinear optical properties were elucidated.

2 EXPERIMENTAL

Silicate glass-based optical fibers: Tm^{3+}/Nd^{3+} codoped fiber, Tm^{3+} doped fiber and Nd^{3+} doped fiber, were drawn from the preforms fabricated by a modified chemical vapour deposition (MCVD) process. The rare earth ions were incorporated into the core of the preforms using conventional solution doping method. The optical parameters of the fibers are listed in Table 1.

Table 1: The optical parameters, viz., refractive index difference between the core and the cladding (Δn), core diameter (d) and cutoff wavelength (λ_c), of the Tm^{3+} doped, the Nd^{3+} doped and the Tm^{3+}/Nd^{3+} codoped optical fibers.

Fiber name	Concentration (M%)	Δn	d (μm)	λ_c (μm)
Tm^{3+} doped	0.03 of Tm	0.0020	7.20	0.79
Nd^{3+} doped	0.03 of Nd	0.0051	8.44	1.34
Tm^{3+}/Nd^{3+} codoped	0.10 of Tm 0.05 of Nd	0.0039	7.52	1.25

The absorption spectra of the fibers were measured by the cutback method using optical spectrum analyzer (OSA) and white light source. To measure emission spectrum, the fibers were excited by a He-Ne laser (Melles Griot 9132EW-1) operating at 633 nm and the spectral output power was detected by an OSA. The fluorescent lifetime of the Tm^{3+}/Nd^{3+} codoped fiber was detected by an InGaAs photo-detector, while ${}^4F_{3/2}$ level of Nd^{3+} was excited by a cw-Ti:sapphire laser (Mira-900, Coherent) operating at 800 nm.

To determine the nonlinear optical parameters, wavelength dependence of refractive indices of the Tm^{3+}/Nd^{3+} codoped fiber preform was measured by using a prism coupler (Sairon: SPA-4000). To avoid unnecessary measurement error due the relatively small core of the fiber preform (0.97 mm), the obtained refractive index results were compared with those of the GeO_2 doped SiO_2 glass, whereas both have GeO_2 concentration of nearly 3.1 M% (Kobayashi et al., 1977); (Kobayashi et al., 1978). Note that the refractive indices were taken by assuming that effect of Tm^{3+} and Nd^{3+} on them is negligible due to their low concentrations.

3 THEORY

The measured line strength of the selected band can be determined by (Judd, 1962):

$$S_{med}(J \rightarrow J') = \frac{3ch(2J+1)n}{8\pi^3 \lambda_{peak} e^2 N}\left[\frac{9}{(n^2+2)^2}\right]\Gamma \qquad (1)$$

where J and J' are the total angular momentum quantum numbers of initial and final states, respectively. c, h, n, λ_{peak}, e, N and Γ are the velocity of light, the Plank constant, the refractive index of glass, the peak absorption wavelength, the charge of the electron, the ion concentration and the integrated absorption coefficient, respectively.

Then, the calculated line strength, which depends on three parameters known as the JO parameters (Ω_t, t = 2, 4, 6), is defined as:

$$S_{cal}(J \rightarrow J') = \sum_{(t=2,4,6)} \Omega_t \left|\left\langle J \left\| U^{(t)} \right\| J' \right\rangle\right|^2. \qquad (2)$$

In our calculations, $\left|\left\langle J \left\| U^{(t)} \right\| J' \right\rangle\right|^2$, the value of the double reduced matrix elements, was taken from Carnall et al. (Carnall et al., 1968). The radiative transition probability (A), the radiative lifetime (τ_r) and the fluorescence branching ratio (β) are described as:

$$A(J \rightarrow J') = \frac{64\pi^4 e^2 n(n^2+2)^2}{3h\lambda_{peak}^3 (2J+1)9} S_{cal}(J \rightarrow J'), \qquad (3)$$

$$\tau_r = \frac{1}{\sum A(J \rightarrow J')} \text{ and} \qquad (4)$$

$$\beta(J \rightarrow J') = \frac{A(J \rightarrow J')}{\sum A(J \rightarrow J')} = A(J \rightarrow J')\tau_r. \qquad (5)$$

The emission cross-sections were determined by the Fuchtbauer-Ladenburg (FL) relation (Aull and Jenssen, 1982); (Fowler and Dexter, 1962); (Krupke, 1974) using the radiative parameters and the effective line width ($\Delta\lambda_{eff}$) as follows:

$$\sigma_e(\lambda_{peak}) = \frac{\lambda_{peak}^4 A(J \rightarrow J')}{8\pi c n^2 \Delta\lambda_{eff}}. \qquad (6)$$

The nonlinear optical parameters, viz., Abbe number (ν_e), nonlinear refractive index (n_2), nonlinear refractive index coefficient (γ) and susceptibility (χ), were evaluated by the following equations (Boling and Glass, 1978); Milam and Weber, 1976); (Weber et al., 1983):

$$\nu_e = \frac{n_e - 1}{n_f - n_c}, \tag{7}$$

$$n_2 = \frac{68(n_e - 1)(n_e^2 + 2)^2}{\nu_e \sqrt{1.517 + \frac{(n_e^2 + 2)(n_e + 1)\nu_e}{6 n_e}}}, \tag{8}$$

(in 10^{-13} esu)

$$\gamma = 4\pi \times 10^3 n_2 / (c n_e) \text{ (in m}^2\text{/W) and} \tag{9}$$

$$\chi = \left(\frac{4}{3}\right) \gamma c n_e^2 \varepsilon_0 \text{ (in m}^2\text{/ V}^2\text{)} \tag{10}$$

where n_e, n_f and n_c are the refractive indices at 546.1, 480, and 643.8 nm, respectively; ε_0 is the permittivity of free space.

4 RESULTS AND DISCUSSION

4.1 Absorption Spectrum

The absorption spectrum of the Tm^{3+}/Nd^{3+} codoped fiber measured over the wavelength range of 400–1700 nm with corresponding electronic energy levels is shown in Figure 1. As a comparison, the absorption spectra of the Tm^{3+} doped and the Nd^{3+} doped fibers are shown in Figure 2. In the absorption spectrum of the Tm^{3+}/Nd^{3+} codoped fiber, the absorption bands of Tm^{3+} and Nd^{3+} were overlapped as follows:

(i) 466 nm, Tm^{3+}: $^3H_6 \rightarrow {}^1G_4$ and Nd^{3+}: $^4I_{9/2} \rightarrow {}^2K_{15/2}+{}^4G_{11/2}+{}^2D_{3/2}+{}^2G_{9/2}$,
(ii) 679 nm, Tm^{3+}: $^3H_6 \rightarrow {}^3F_2+{}^3F_3$ and Nd^{3+}: $^4I_{9/2} \rightarrow {}^4F_{9/2}$,
(iii) 784 nm, Tm^{3+}: $^3H_6 \rightarrow {}^3H_4$ and Nd^{3+}: $^4I_{9/2} \rightarrow {}^2H_{9/2}+{}^4F_{5/2}$,
(iv) 1575 nm, Tm^{3+}: $^3H_6 \rightarrow {}^3F_4$ and Nd^{3+}: $^4I_{9/2} \rightarrow {}^4I_{15/2}$.

Among them, the absorption intensity of the peak at 784 nm was higher than that of the others, since it was a combination of the strong absorption of Tm^{3+}: $^3H_4$ and Nd^{3+}: $^2H_{9/2}+{}^4F_{5/2}$ levels (Rakov et al., 2009). In addition, the Tm^{3+}/Nd^{3+} codoped fiber illustrated five well separated absorption bands. The bands were composed of a single separated absorption band of Tm^{3+} at 1212 nm ($^3H_6 \rightarrow {}^3H_5$ transition) and four separated absorption bands of Nd^{3+} located at 528, 582, 750 and 889 nm. They are corresponding to the transitions from $^4I_{9/2}$ to $^2K_{13/2}+ {}^4G_{7/2}$, $^4G_{5/2}+ {}^2G_{7/2}$, $^4S_{3/2}+{}^4F_{7/2}$ and $^4F_{3/2}$, respectively.

In the case of the Nd^{3+} doped fiber, the absorption intensity of the peak at 582 nm was stronger than that of the others since it is dominant in silicate glasses (Stokowski et al., 1981); (Thomas et al., 1992), whereas for fluoride glasses it is comparable with that of 800 nm (Binnemans et al., 1998); (Digonnet, 1993); (Lucas et al., 1978). Since the absorption peak locations of Nd^{3+} at 750 nm ($^4S_{3/2}+{}^4F_{7/2}$) and 810 nm ($^2H_{9/2}+{}^4F_{5/2}$) were close to the absorption peak of Tm^{3+} at 791 nm ($^3H_4$, in Figure 2) (Chung et al., 1997), absorption bands located around 750 and 784 nm seemed to be overlapped each other in the codoped fiber as illustrated in Figure 1. Note that the peaks around 1383 nm indicated the presence of OH ions in the core of the fibers.

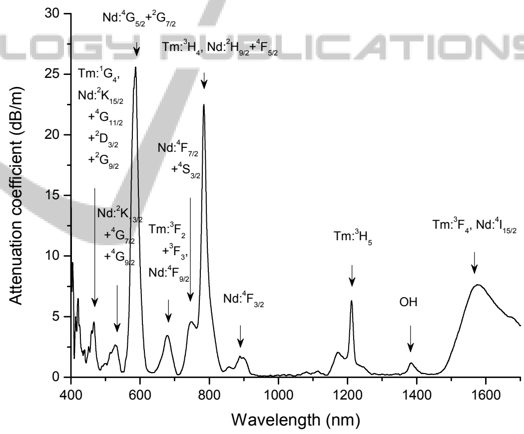

Figure 1: Absorption spectrum of the Tm^{3+}/Nd^{3+} codoped optical fiber.

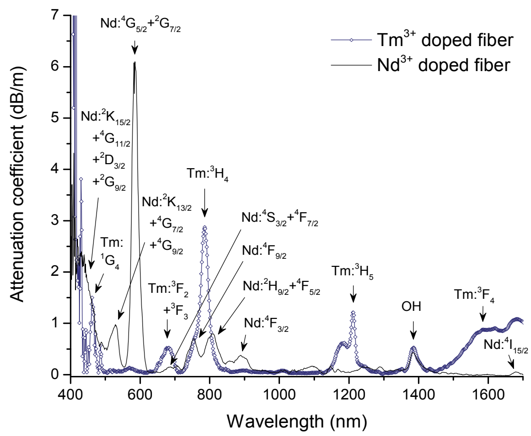

Figure 2: Absorption spectra of the Tm^{3+} doped and the Nd^{3+} doped optical fibers.

4.2 Emission Spectrum

In the absorption spectrum of the Tm^{3+}/Nd^{3+} codoped fiber, two obvious absorption bands existed at 582 and 784 nm. The former was the absorption of Nd^{3+} alone, but the latter was the absorption of both Nd^{3+} and Tm^{3+}. Therefore, the 582 nm absorption band was selected as a pump band to investigate an ET from Nd^{3+} to Tm^{3+}. The commercially available He-Ne laser was used to excite Nd^{3+} ions in the fiber core by coupling the laser light at 620 and 633 nm into the fiber core with the power of 0.01 and 4.4 mW, respectively.

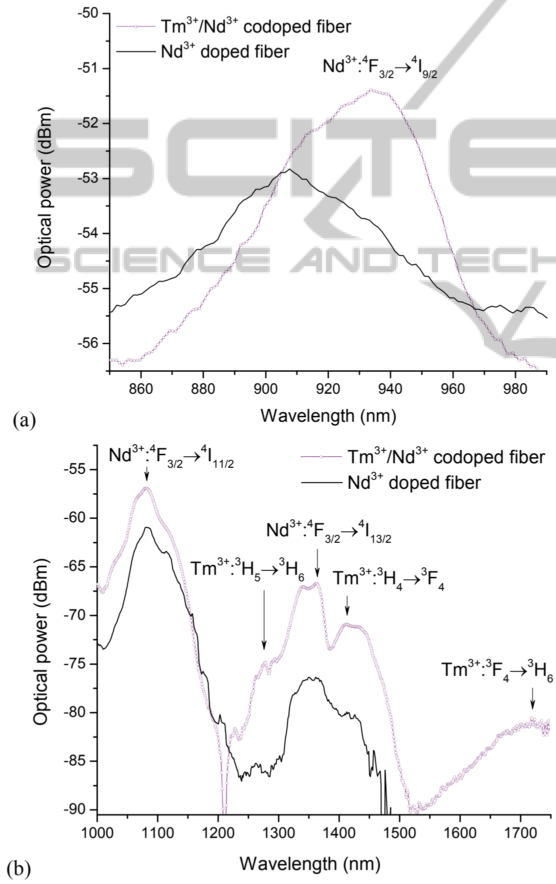

Figure 3: Emission spectra of the Tm^{3+}/Nd^{3+} codoped and the Nd^{3+} doped fibers upon pumping with He-Ne laser at 633 nm over the wavelength range of (a) 850–990 nm and (b) 1000–1750 nm. The fiber lengths used were 20 m.

The NIR emission spectrum of the Tm^{3+}/Nd^{3+} codoped fiber comparing with that of the Nd^{3+} doped fiber upon pumping at 633 nm is shown in Figure 3. The emission bands appeared at 934, 1083 and 1362 nm from Nd^{3+} ions in the Tm^{3+}/Nd^{3+} codoped fiber. Another emission bands from Tm^{3+} also appeared at 1279, 1414 and 1720 nm. On account of the emissions contributed from Nd^{3+}, the NIR emission spectrum of the Tm^{3+}/Nd^{3+} codoped fiber was broadened from 1215 to 1515 nm. On the other hand, the Nd^{3+} doped fiber showed the emission bands only at 934, 1083 and 1362 nm (Zhang et al., 2006) by exciting at 633 nm. No emission band was observed in the Tm^{3+} doped fiber upon pumping at 633 nm.

Figure 4 illustrates the electronic energy level diagram of Tm^{3+} and Nd^{3+} ions. The mechanism of the emission and ET process can be explained as follows. When the Tm^{3+}/Nd^{3+} codoped fiber was pumped at 633 nm, Nd^{3+} ions from the ground state ($^4I_{9/2}$) were excited to $^4G_{5/2}+^2G_{7/2}$ and subsequently, decayed to the $^4F_{3/2}$ metastable state. The emission bands of Nd^{3+} appeared at 934, 1083 and 1362 nm correspond to the transitions from $^4F_{3/2}$ to $^4I_{9/2}$, $^4I_{11/2}$, and $^4I_{13/2}$, respectively. Because of the presence of competing emissions from the same level ($^4F_{3/2}$), the emission intensity of the peak at 1362 nm was not as strong as that at 934 and 1083 nm (Choi et al., 2003); (Zhang et al., 2006). In addition, after the fast nonradiative decay processes, the ET process took place between two excited levels Nd^{3+}: $^4F_{3/2}$ and Tm^{3+}: $^3H_4$. These two energy levels matched with the estimated energy gap of about 1□10^3 cm^{-1} (Tanabe et al., 2000).

As a result of the ET process, the Tm^{3+}/Nd^{3+} codoped fiber showed the emissions of Tm^{3+} around 1279, 1414 and 1720 nm. They are related to the radiative decay from $^3H_5 \rightarrow {}^3H_6$, $^3H_4 \rightarrow {}^3F_4$ and $^3F_4 \rightarrow {}^3H_6$ transitions, respectively. The emission spectrum over the wavelength of 1750 nm was not possible to detect due to the limitation of the OSA.

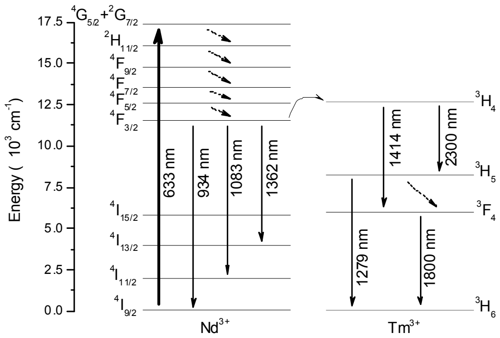

Figure 4: Schematic electronic energy levels and transitions of Tm^{3+} and Nd^{3+} ions upon exciting at 633 nm. Bold arrow, solid thin arrows, curved arrow and dashed arrows represent the pump wavelength, the emission wavelengths, the ET process and the nonradiative decays, respectively.

4.3 JO Parameters

The JO analysis was applied using the absorption bands of Nd^{3+} in the Tm^{3+}/Nd^{3+} codoped optical fiber to characterize its spectroscopic properties. The concentration of Tm^{3+} and Nd^{3+} in the Tm^{3+}/Nd^{3+} codoped optical fiber was approximately taken as 1.76×10^{25} m^{-3} and 0.91×10^{25} m^{-3}, respectively. They were estimated from the Tm^{3+} doped and the Nd^{3+} doped optical fiber fabricated by modified solution doping method (Han and Kim, 2002). The values of the JO parameters were, respectively, 8.16×10^{-24}, 3.20×10^{-24} and 2.67×10^{-24} m^2 for Ω_2, Ω_4 and Ω_6. The JO intensity parameters of the present work compared with the results of the Tm^{3+}/Nd^{3+} codoped glasses (Brandão et al., 2006); (Chung and Heo, 2001), the Tm doped fibers (Peterka et al., 2004); (Walsh and Barnes, 2004), and the Nd doped fiber preform and glass (Martinez et al., 1998); (Thomas et al., 1992) are listed in Table 2.

The JO parameters obtained in the present work indicated the trend as $\Omega_2 > \Omega_4 > \Omega_6$ as the same trend has been found in previous reports (Chung and Heo, 2001); (Martinez et al., 1998); (Thomas et al., 1992); (Walsh and Barnes, 2004). Nevertheless, the trend of the Tm^{3+}/Nd^{3+} codoped glass (Brandão et al., 2006) showed higher Ω_6 than Ω_4 ($\Omega_2 > \Omega_6 > \Omega_4$). Since the intensity parameter (Ω_2) is related to the degree of covalence (Digonnet, 1993), the large value of Ω_2 in the present work indicates the presence of covalent bonding between Tm^{3+} and Nd^{3+}. It is known that ionic metals like fluoride and fluorophosphates glasses have very small values of Ω_2 (Binnemans et al., 1998), whereas covalent materials like silicate glasses have large values. Ω_6 is related to the rigidity of material and the higher ratio of Ω_4/Ω_6 (= 1.2) implies that the Tm^{3+}/Nd^{3+} codoped fiber possessed a good spectroscopic quality.

4.4 The Spectroscopic and Nonlinear Optical Parameters

The values of line strengths and absorption cross-sections from the transitions of $^4I_{9/2}$ to respective higher energy levels are listed in Table 3. The rms deviation (Yanbo et al., 2006) of the calculated and measured absorption line strengths was 2.99×10^{-25} m^2. The spectroscopic parameters of the Tm^{3+}/Nd^{3+} codoped fiber are summarized in Table 4. In the transitions of Tm^{3+}, the radiative transition probabilities were dominated by $^3H_4 \rightarrow {}^3H_6$ transition. In addition, $^3H_5 \rightarrow {}^3H_6$ and $^3F_4 \rightarrow {}^3H_6$ transitions had strong line strengths and radiative transition probabilities which were the good evidence of the emissions of Tm^{3+} around 1279 nm (Yang, et al., 2006) and 1720 nm (Zou and Toratani, 1996). For the spectroscopic parameters of Nd^{3+}, $^4F_{3/2} \rightarrow {}^4I_{11/2}$ transition was more dominant than that of the others (Digonnet, 1993).

The branching ratios of the Tm^{3+}/Nd^{3+} codoped fiber hold the same significance as previous reports (Stokowski et al., 1981); (Thomas et al., 1992); (Walsh and Barnes, 2004); (Watekar et al., 2006). For the transitions originated from $^3H_4$ level of Tm^{3+}, the $^3H_4 \rightarrow {}^3H_5$ transition indicates the smallest branching ratios (1.57%). Therefore, the $^3H_5$ level was not well populated and the emission efficiency of 1279 nm was generally smaller than that of 1414 nm (Heo et al., 1997). In general, Nd^{3+} doped silica glass favours the $^4F_{3/2} \rightarrow {}^4I_{11/2}$ transition and the branching ratio of it is closed to 50%.

When comparing the radiative lifetimes of the Tm^{3+}/Nd^{3+} codoped fiber with those of previous studies, the radiative lifetimes of Tm^{3+} at $^3H_5$ and $^3F_4$ levels agreed well with those found by others (Peterka et al., 2004); (Walsh and Barnes, 2004), whereas the radiative lifetime of Tm^{3+} at $^3H_4$ level was slightly lower than that reported in previous studies (Peterka et al., 2004); (Walsh and Barnes, 2004); (Watekar et al., 2006). Moreover, the radiative lifetime of upper level ($^3H_4$, 0.54 ms) was too short to achieve the desired population inversion than that of the lower level ($^3F_4$, 3.70 ms). This is normally termed a self-terminating transition (Quimby and Miniscalco, 1989). As a result, in the glasses doped with Tm^{3+} only, the population inversion is not possible under 800 nm excitation and the emission spectrum was hardly recorded (Lee et al., 2003). In the case of the radiative lifetime of Nd^{3+} in the Tm^{3+}/Nd^{3+} codoped fiber, that of $^4F_{3/2}$ level was found to increase (Lu and Dutta, 2001); (Thomas et al., 1992); Yanbo et al., 2006). It is noted that the molar ratio of Tm^{3+} to Nd^{3+} (= 2) was a clear evidence of the optimum composition to deplete the clustering of the Nd^{3+} ions (Chung et al., 1997). Since the clustering effect causes fast decay in the emission spectrum, it decreases the total radiative lifetime (Lu and Dutta, 2001).

The fluorescence lifetime of $^4F_{3/2}$ level in the Tm^{3+}/Nd^{3+} codoped fiber upon exciting at 800 nm was 0.56 ms. It was more than or nearly equal to that reported by others (Krupke, 1974); (Stokowski et al., 1981); (Thomas et al., 1992). Nonradiative lifetime ($^4F_{3/2}$ level) and radiative quantum efficiency (Krupke, 1974) of the Tm^{3+}/Nd^{3+} codoped fiber were 0.67 ms and 0.17, respectively. Because of the poor

Table 2: Comparison of the JO parameters in different types of materials.

JO parameter (10^{-24} m^2)	Present work	Tm^{3+}/Nd^{3+} codoped glass (Brandão, et al., 2006)	Tm^{3+}/Nd^{3+} codoped glass* (Chung & Heo, 2001)	Tm doped fiber (Peterka, et al., 2004)	Tm doped fiber (Walsh & Barnes, 2004)	Nd doped fiber preform (Martinez, et al., 1998)	Nd doped glass (Thomas, et al., 1992)
Ω_2	8.16 ± 0.30	7.28	3.74	3.26	6.23	5.81	9.31
Ω_4	3.20 ± 0.13	4.55	1.43	1.20	1.91	3.80	4.13
Ω_6	2.67 ± 0.23	6.18	1.09	0.46	1.36	2.42	3.91

*The JO intensity parameters were taken from Tm^{3+} doped glasses.

Table 3: The values of absorption cross-section (σ_a), measured line strength (S_{med}) and calculated line strength (S_{cal}) estimated based on the absorption bands of Nd^{3+} in the Tm^{3+}/Nd^{3+} codoped fiber.

Transitions (from $^4I_{9/2}$)	λ_{peak} (nm)	n (λ)	σ_a (10^{-25} m^2)	S_{med} (10^{-24} m^2)	S_{cal} (10^{-24} m^2)	$(\Delta S)^2$ (10^{-50} m^4)
$^2K_{13/2}+^4G_{7/2}+^4G_{9/2}$	528	1.481	4.38	1.58	1.58	0.00
$^4G_{5/2}+\ ^2G_{7/2}$	582	1.473	23.12	10.29	10.03	6.76
$^4F_{7/2}+^4S_{3/2}$	750	1.460	4.32	1.77	1.91	1.96
$^4F_{3/2}$	889	1.453	1.03	0.83	0.88	0.25

Table 4: The spectroscopic parameters, viz., calculated line strength (S_{cal}), radiative transition probabilities ($A_{JJ'}$), fluorescence branching ratios ($\beta_{JJ'}$), radiative lifetimes (τ_r), effective linewidths ($\Delta\lambda_{eff}$) and emission cross-sections (σ_e), of the Tm^{3+}/Nd^{3+} codoped fiber estimated along with peak emission wavelengths.

	Transitions	λ_{peak} (nm)	n (λ)	S_{cal} (10^{-24} m^2)	$A_{JJ'}$ (s^{-1})	$\beta_{JJ'}$ (%)	τ_r (ms)	$\Delta\lambda_{eff}$ (nm)	σ_e (10^{-25} m^2)
Tm^{3+}	$^3H_5 \rightarrow\ ^3H_6$	1279	1.446	3.32	281.01	98.64	3.51	35.33	13.50
	$^3H_5 \rightarrow\ ^3F_4$	3870	1.434	1.30	3.87	1.36		-	-
	$^3H_4 \rightarrow\ ^3H_6$	800	1.457	3.87	1674.71	90.14	0.54	-	-
	$^3H_4 \rightarrow\ ^3F_4$	1414	1.444	2.02	154.11	8.29		61.08	6.41
	$^3H_4 \rightarrow\ ^3H_5$	2300	1.440	1.66	29.10	1.57		-	-
	$^3F_4 \rightarrow\ ^3H_6$	1800	1.442	7.35	270.18	100.00	3.70	-	-
Nd^{3+}	$^4F_{3/2} \rightarrow\ ^4I_{9/2}$	934	1.452	0.88	532.40	42.92	0.81	55.50	4.59
	$^4F_{3/2} \rightarrow\ ^4I_{11/2}$	1083	1.449	1.54	594.16	47.90		59.32	8.71
	$^4F_{3/2} \rightarrow\ ^4I_{13/2}$	1362	1.445	0.57	108.92	8.78		49.61	4.80
	$^4F_{3/2} \rightarrow\ ^4I_{15/2}$	1940	1.441	0.07	4.94	0.40		-	-

Table 5: Abbe number (ν_e), nonlinear refractive index (n_2), nonlinear refractive index coefficient (γ) and susceptibility (χ) of the Tm^{3+}/Nd^{3+} codoped fiber comparing with the results reported previously.

	n_e	ν_e	n_2 (10^{-13} esu)	γ (10^{-4} m^2/W)	χ (10^{-6} m^2/ V^2)
Present work	1.478	20.0	5.69	1.61	1.25
Yb^{3+}/Tm^{3+} codoped glass (Watekar, et al., 2005)	-	55.6	1.35	0.38	0.30
Nd doped glass (Stokowski, et al., 1981)	1.720	45.0	3.44	-	-

emission intensity of the fiber upon exciting at 800 nm, the fluorescence lifetime of Tm^{3+} was not possible to observe.

The effective linewidths of Tm^{3+} from $^3H_5 \rightarrow\ ^3H_6$ and $^3H_4 \rightarrow\ ^3H_5$ transition reported by other groups (Balda et al., 2008); (Yang et al., 2006); (Zhou et al., 2010) were broader by nearly 30 nm than the values estimated here. Nevertheless, the emission cross-sections of Tm^{3+} were found to increase significantly (Balda et al., 2008); (Yang, et al., 2006). On the other hand, in the case of Nd^{3+} the effective linewidths were larger but the peak emission cross-sections were smaller (Stokowski et al., 1981); (Thomas et al., 1992) since the decrease of the emission cross-section is mainly due to the increase of the effective linewidths (Choi et al., 2003).

The nonlinear optical parameters of the Tm^{3+}/Nd^{3+} codoped fiber comparing with that of the Yb^{3+}/Tm^{3+} codoped glass (Watekar et al., 2005) and the Nd doped glass (Stokowski et al., 1981) are listed in Table 5. The calculated results showed low Abbe number and reasonably high nonlinear refractive index (Boling and Glass, 1978). Therefore, the Tm^{3+}/Nd^{3+} codoped fiber can also be applied to the development of future phase and amplitude modulators and fast all-optical switches for communication (Digonnet, 1993).

5 CONCLUSIONS

We fabricated the Tm^{3+}/Nd^{3+} codoped optical fiber by the MCVD process. The fiber was excited by the He-Ne laser operating at 633 nm and the emissions were found to appear at 934, 1083, 1279, 1363, 1414 and 1720 nm. The emission bands of Tm^{3+} at 1279, 1414 and 1720 nm assured the ET process between Tm^{3+} and Nd^{3+} ions. The process was so beneficial that the Tm^{3+}/Nd^{3+} codoped fiber can be good candidate for the broadband fiber laser in NIR region. In addition, the trend of the JO parameters ($\Omega_2 > \Omega_4 > \Omega_6$) indicated that the Tm^{3+}/Nd^{3+} codoped fiber occupied a good spectroscopic quality. Further, higher radiative lifetime and larger effective linewidths originated from $^4F_{3/2}$ level as well as considerably large stimulated emission cross-sections at 1279 and 1414 nm were observed in the Tm^{3+}/Nd^{3+} codoped fiber. Furthermore, the nonlinear optical parameters of the fiber were calculated and the considerably highly nonlinear refractive index was found.

ACKNOWLEDGEMENTS

This work was supported partially by the Ministry of Science and Technology, the New Growth Engine Industry Project of the Ministry of Knowledge Economy, the Core Technology Development Program for Next-generation Solar Cells of Research Institute of Solar and Sustainable Energies, National Research Foundation of Korea (NRF) grant funded by the Korea government (MEST) (No. 2011-0031840), the Brain Korea-21 Information Technology Project, and by the (Photonics 2020) research project through a grant provided by the Gwangju Institute of Science and Technology in 2012, South Korea.

REFERENCES

Aull, B. & Jenssen, H., 1982. Vibronic interactions in Nd:YAG resulting in nonreciprocity of absorption and stimulated emission cross sections. IEEE J. Quantum Electron., vol. 18, no. 5, pp. 925-930.

Balda, R. et al., 2008. Spectroscopic properties of the 1.4 µm emission of Tm^{3+} ions in TeO_2-WO_3-PbO glasses. Opt. Express, vol. 16, no. 16, pp. 11836-11846.

Binnemans, K., Deun, R. V., Gorller-Walrand, C. & Adam, J.L., 1998. Optical properties of Nd^{3+}-doped fluorophosphate glasses. J. Alloy. Compd., vol. 275-277, pp. 455-460.

Boling, N. L. & Glass, A. J., 1978. Empirical relationships for predicting nonlinear refractive index changes in optical solids. IEEE J. Quantum Electron., vol. 14, no. 8, pp. 601-608.

Brandão, M. J. S. et al., 2006. Optical properties and energy transfer processes in (Tm^{3+}, Nd^{3+}) doped tungstate fluorophosphate glass. J. Appl. Phys., vol. 99, no. 11, p. 113525.

Carnall, W. T., Fields, P. R. & Rajnak, K., 1968. Spectral intensities of the trivalent lanthanides and actinides in solution. II. Pm^{3+}, Sm^{3+}, EU^{3+}, Gd^{3+}, Tb^{3+}, Dy^{3+} and Ho^{3+}. J. Chem. Phys., vol. 49, no. 10, pp. 4412-4423.

Choi, J. H. et al., 2003. Optical absorption and emission properties of Nd^{3+} doped fluorophosphates glass for broadband fiber amplifier applications. Proc. SPIE, vol. 4974, pp. 106-111.

Chung, W. J. & Heo, J., 2001. Energy transfer process for the blue up-conversion in calcium aluminate glasses doped with Tm^{3+} and Nd^{3+}. J. Am. Ceram. Soc., vol. 84, no. 2, pp. 384-352.

Chung, W. J., Yoo, J. R., Kim, Y. S. & Heo, J., 1997. Mechanism of the blue up-conversion in Tm^{3+}/Nd^{3+}-doped calcium aluminate glasses. J. Am. Ceram. Soc., vol. 80, no. 6, pp. 1485-1490.

Fowler, W. B. & Dexter, D. L., 1962. Relation between absorption and emission probabilities in luminescent centers in ionic solids. Phys. Rev., vol. 128, pp. 2154-2165.

Digonnet, M. J. F. (ed.), 1993. *Rare-earth-doped fiber lasers and amplifiers*. Marcel Dekker, Inc.

Han, W.-T. & Kim, Y. H., 2002. Linear and nonlinear optical properties of optical fibers containing PbTe quantum dots for all optical switching application. *2nd Int. China-Korea Glass and Glass-Ceramics Symp.*, Shanghi.

Heo, J., Cho, W. Y. & Chung, W. J., 1997. Sensitizing effect of Tm^{3+} on 2.9 µm emission from Dy^{3+}-doped Ge_{25} Ga_5 S_{70} glass. J. Non-Cryst. Solids, vol. 212, pp. 151-156.

Judd, B. R., 1962. Optical absorption intensities of rare-earth ions. Phy. Rev., vol. 127, pp. 750-761.

Kobayashi, S., Shibata, N., Shibata, S. & Izawa, T., 1978. Characteristics of optical fibers in infrared wavelength region. Review of ECL, vol. 26, no. 3, pp. 453-467.

Kobayashi, S., Shibata, S., Shibata, N. & Izawa, T., 1977. Refractive-index dispersion of doped fused silica. *1stInternational Conference on Integrated Optics and Optical Fiber Communication (IECE)*, Tokyo.

Krupke, W. F., 1974. Induced-emission cross sections in neodymium laser glasses. *IEEE J. Quantum Electron.*,

vol. QE-10, no. 4, pp. 450-457.
Lahoz, F., Shepherd, D. P., Wilkinson, J. S. & Hassan, M. A., 2008. Efficient blue upconversion emission due to confined radiative energy transfer in Tm^{3+}–Nd^{3+} co-doped Ta_2O_5 waveguides under infrared-laser excitation. Opt. Commun., vol. 281, pp. 3691-3694.
Lee, D. J., Heo, J. & Park, S. H., 2003. Energy transfer and 1.48 μm emission properties in chalcohalide glasses doped with Tm^{3+} and Tb^{3+}. J. Non-Cryst. Solids, vol. 331, pp. 181-189.
Lucas, J. et al., 1978. Preparation and optical properties of neodymium fluorozirconate glasses. J. Non-Cryst. Solids, vol. 27, pp. 273-283.
Lu, K. & Dutta, N. K., 2001. Spectroscopic properties of Nd-doped glass for 944 nm laser emission. J. Appl. Phys., vol. 89, no. 6, pp. 3079-3083.
Martinez, A., Zenteno, L. A. & Kuo, J. C. K., 1998. Optical and spectroscopic characterization of Nd-doped aluminosilicate fiber preforms made by the MCVD method using chelate delivery. Appl. Phys. B, vol. 67, pp. 17-21.
Milam, D. & Weber, M. J., 1976. Measurement of nonlinear refractive-index coefficients using time-resolved interferometry: application to optical materials for high-power neodymium lasers. J. Appl. Phys., vol. 47, pp. 2497-2501.
Peterka, P. et al., 2004. Theoretical modelling of S-band thulium-doped silica fibre amplifiers. Opt. Quant. Electron., vol. 36, pp. 201-212.
Quimby, R. S. & Miniscalco, W. J., 1989. Continuous-wave lasing on a self-terminating transition. Appl. Opt., vol. 28, no. 1, pp. 14-16.
Rakov, N., Gómez, L. A., Rátiva, D. J. & Maciel, G. S., 2002. Blue upconversion enhancement by a factor of 200 in Tm^{3+}-doped tellurite glass by codoping with Nd^{3+} ions. J. Appl. Phys., vol. 92, no. 10, pp. 6337-6339.
Rakov, N., Gómez, L. A., Rátiva, D. J. & Maciel, G. S., 2009. Blue upconversion emission from Tm^{3+} sensitized by Nd^{3+} in aluminum oxide crystalline ceramic powders. Appl. Phys. B, vol. 94, pp. 199-202.
Shen, S. et al., 2002. Tellurite glasses for broadband amplifiers and integrated optics. J. Am. Ceram. Soc., vol. 85, no. 6, pp. 1391-1395.
Stokowski, S. E., Saroyan, R. A. & Weber, M. J., 1981. Nd-doped laser glass spectroscopic and physical properties. Lawrence Livermore National Laboratory, M-095, Rev. 2, 1.
Tanabe, S., 2002. Rare-earth-doped glasses for fiber amplifiers in broadband telecommunication. C. R. Chim., vol. 5, no. 5, pp. 815-824.
Tanabe, S., Feng, X. & Hanada, T., 2000. Improved emission of Tm^{3+} doped glass for a 1.4-μm amplifier by radiative energy transfer between Tm^{3+} and Nd^{3+}. Opt. Lett., vol. 25, no. 11, pp. 817-819.
Thomas, I. M., Payne, S. A. & Wilke, G. D., 1992. Optical properties and laser demonstrations of Nd-doped sol-gel silica glasses. J. Non-Cryst. Solids, vol. 151, no. 3, pp. 183-194.
Walsh, B. M. & Barnes, N. P., 2004. Comparison of Tm:ZBLAN and Tm:silica fiber lasers; spectroscopy and tunable pulsed laser operation around 1.9 μm. Appl. Phys. B, vol. 78, pp. 325-333.
Watekar, P. R., Ju, S., Boo, S. & Han, W.-T., 2005. Linear and non-linear optical properties of Yb^{3+}/Tm^{3+} co-doped alumino-silicate glass prepared by sol-gel method. J. Non-Cryst. Solids, vol. 351, pp. 2446-2452.
Watekar, P. R., Ju, S. & Han, W.-T., 2006. A small-signal power model for Tm-doped silica-glass optical fiber amplifier. IEEE Photon. Technol. Lett., vol. 18, no. 19, pp. 2035-2037.
Weber, M. J., Lynch, J. E., Blackburn, D. H. & Cronin, D. J., 1983. Dependence of the stimulated emission cross section of Yb^{3+} on host glass composition. IEEE J. Quantum Electron., vol. 19, pp. 1600-1608.
Yanbo, Q. et al., 2006. Spectroscopic properties of Nd^{3+}-doped high silica glass prepared by sintering porous glass. J. Rare Earth., vol. 24, pp. 765-770.
Yang, Z., Luo, L. & Chen, W., 2006. The 1.23 and 1.47 μm emissions from Tm^{3+} in chalcogenide glasses. J. Appl. Phys., vol. 99, no. 7, pp. 076107-3.
Zabicky, J. (ed.), 2009. *The chemistry of metal enolates, part 1*. John Wiley & Sons Ltd.
Zhang, J., Chung, W. J., Zhao, X. & Heo, J., 2010. Nd^{3+} sensitized blue upconversion luminescence in Nd^{3+}/Pr^{3+} co-doped Ge–Ga–S–CsBr chalcohalide glasses. J. Non-Cryst. Solids, vol. 356, pp. 2406-2408.
Zhang, J. W. et al., 2006. Optical amplification in Nd^{3+} doped electro-optic lanthanum lead zirconate titanate ceramics. Appl. Phys. Lett., vol. 89, pp. 061113.
Zhou, B., Lin, H. & Pun, E.Y.-B., 2010. Tm^{3+}-doped tellurite glasses for fiber amplifiers in broadband optical communication at 1.20 μm wavelength region. Opt. Express, vol. 18, no.18, pp. 18805-18810.
Zou, X. & Toratani, H., 1996. Spectroscopic properties and energy transfers in Tm^{3+} singly- and Tm^{3+}/Ho^{3+} doubly-doped glasses. J. Non-Cryst. Solids, vol. 195, pp. 113-124.